

Mechanisms for Flavin-Mediated Oxidation: Hydride or Hydrogen-Atom Transfer?

Felipe Curtolo and Guilherme M. Arantes*



Cite This: *J. Chem. Inf. Model.* 2020, 60, 6282–6287



Read Online

ACCESS |



Metrics & More

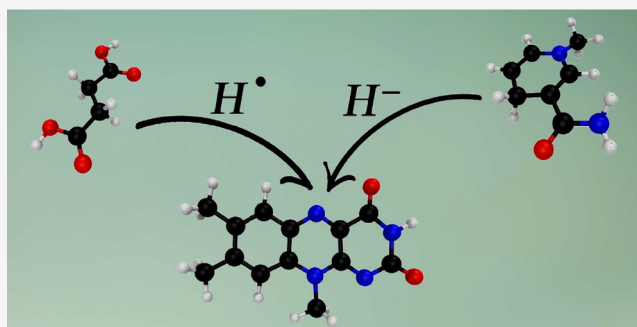


Article Recommendations



Supporting Information

ABSTRACT: Flavins are versatile biological cofactors which catalyze proton-coupled electron transfers (PCET) with varying number and coupling of electrons. Flavin-mediated oxidations of nicotinamide adenine dinucleotide (NADH) and of succinate, initial redox reactions in cellular respiration, were examined here with multiconfigurational quantum chemical calculations and a simple analysis of the wave function proposed to quantify electron transfer along the proton reaction coordinate. The mechanism of NADH oxidation is a prototypical hydride transfer, with two electrons moving concerted with the proton to the same acceptor group. However, succinate oxidation depends on the elimination step and can proceed through the transfer of a hydride or hydrogen atom, with proton and electrons moving to different groups in both cases. These results help to determine the mechanism of fundamental but still debated biochemical reactions and illustrate a new diagnostic tool for electron transfer that can be useful to characterize a broad class of PCET processes.



INTRODUCTION

Enzymes equipped with flavin cofactors comprise the most abundant class of natural catalysts for combined proton and electron transfer.^{1,2} The redox center in all natural flavins is formed by the heteronuclear tricyclic isoalloxazine ring (Figure 1), primarily attached to the protein by noncovalent hydrogen bonds, stacking, and cation- π contacts.^{3–5} These interactions also modulate the flavin redox potential from -400 to 60 mV, allowing oxidation of a range of aliphatic and aromatic substrates.^{6–8}

Flavin redox reactions are an example of proton-coupled electron transfers or PCET, a broad family of reactions and energy conversion processes in chemistry.^{9–11} PCET mechanisms are characterized by the number of electrons involved, such as in hydride ($2e^-/1H^+$) versus hydrogen-atom ($1e^-/1H^+$, or HAT) transfer;¹² the order of steps or their concurrency, such as electron transfer first, proton second (ETPT), or concerted proton-electron transfer (CPET);^{9,13} whether the transfers proceed from(to) the same or different chemical groups in the donor(acceptor), as in multiple-site PCET;^{10,14} and the tunneling behavior and the adiabaticity or participation of excited-states in the transfer processes.^{13,15}

Thermochemical and redox potential measurements determined that flavins may undergo hydride and single-electron ($1e^-$) transfers,^{10,16} and molecular simulations explored their tunneling effects.^{17–20} However, a description of possible HAT, particularly in enzymatic mechanisms, has received less attention.²¹ A remarkable example is the BLUF flavoprotein

which has been shown by ultrafast spectroscopy and simulations to sustain HAT by light activation.^{22,23}

Quantitative diagnostics of PCET mechanisms can be obtained from quantum-chemical calculations of molecular properties along the reaction progress (usually the proton transfer coordinate).¹³ Nonadiabatic couplings¹⁵ and dipole moments²⁴ are well-behaved properties. However, the calculation of partial charges and spins,²⁵ the simplest and most common diagnostic used,^{13,26–28} can be problematic because these are not physical observables and may be calculated with different recipes.^{29–31} Realizing these difficulties, intrinsic bond orbitals³² were recently proposed and successfully applied to identify proton and electron donors in PCET.^{33,34}

Here, we address the PCET mechanism in flavin-mediated oxidation of NADH (reduced nicotinamide adenine dinucleotide) and of succinate catalyzed respectively by respiratory complex I (or type I NADH dehydrogenase)^{35–37} and by complex II (or succinate dehydrogenase, see Figure 1).^{38,39} These fundamental steps for cellular respiration have been traditionally assigned to hydride transfers,^{36,39} but recent

Received: August 13, 2020

Published: November 2, 2020



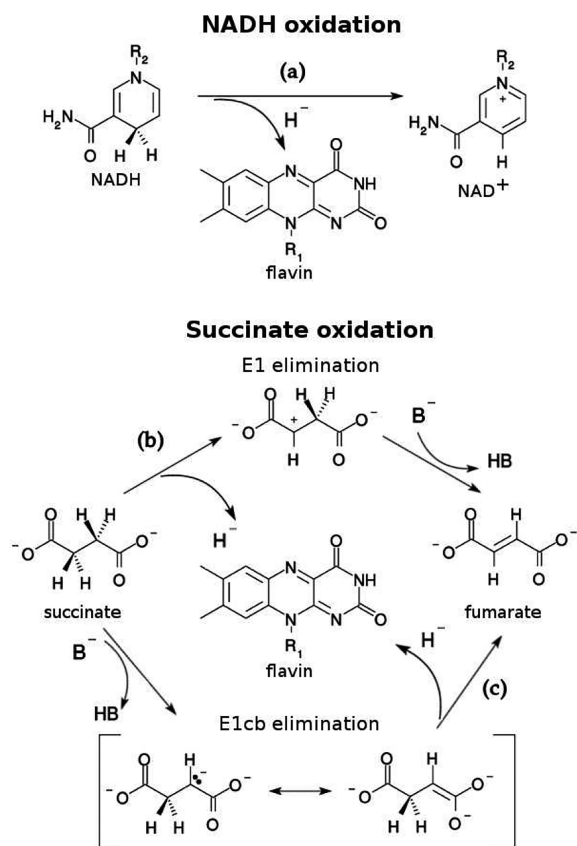


Figure 1. Flavins mediate oxidation of NADH and succinate. NADH reacts by elimination from the nicotinamide ring, step (a). Two reaction sequences are possible for succinate oxidation: unimolecular elimination (E1) is shown in step (b) and conjugate base elimination (E1cb) in step (c). Biologically relevant flavins differ only in the R_1 substituent. R_2 is the ribosyl-ADP moiety, and B^- is a general base.

studies disputed this view and proposed HAT mechanisms.^{26,27}

Computational Methods. The three reactions studied here are models of flavin-mediated oxidations catalyzed by respiratory complexes I and II (Figure 1). The flavin isoalloxazine ring was represented by lumiflavin (LF, IUPAC name 7,8,10-trimethylbenzo[*g*]pteridine-2,4-dione) instead of flavin mononucleotide (FMN) and flavin adenine dinucleotide (FAD) natural cofactors. Ribityl-ADP (adenosine diphosphate) and ribityl-phosphate moieties were replaced by methyl groups. The ribosyl-ADP moiety in NADH was replaced by a methyl group, generating 1-methylnicotinamide in the reduced form (MNAH or 1-methyl-4H-pyridine-3-carboxamide, Figure 2). Succinate had its carboxylates protonated into succinic acid and E1cb elimination from H_2Succ^- [(E)-4-hydroxy-4-oxidobut-3-enoic acid]. This is consistent with the active site in respiratory complex II³⁸ that shields the negative charges in succinate carboxylates by hydrogen bonding with positively charged residues and with previous calculations on similar reactions.⁴⁰ These models had 45, 44, and 51 atoms, respectively.

Molecular geometries were optimized at the MP2 level⁴¹ with the def2-SVP basis set.⁴² Resolution of identity with the def2/J⁴³ and def2-SVP/C⁴⁴ auxiliary basis was used. Optimizations with methods neglecting dispersion interactions resulted in disruption of the experimental^{35,38} stacked orientation between reactants. Transition structures were

confirmed by analysis of the Hessian eigenvector with the negative eigenvalue and of the intrinsic reaction coordinates (Table S1, Supporting Information).⁴⁵

A reaction coordinate $RC = r_1 - r_2$ was defined by the broken bond distance (r_1 , between the transferred H and C2 atom in H_2Succ/H_2Succ^- or C4 atom in MNAH) minus the formed bond distance (r_2 , between H and N5 atom in LF, Figure 2). The reaction profile was obtained with constrained geometry optimizations fixing r_1 while relaxing all others degrees of freedom using the ORCA 4.1.1 program.⁴⁶ Intrinsic bond orbitals (IBOs)³² were obtained from localization³³ of the broken-symmetry solution³⁴ of unrestricted M06⁴⁷ single-point calculations with ORCA.

The complete active space self-consistent field (CASSCF)^{28,41} method was used with the PySCF package version 1.5⁴⁸ for singlet spin states in C_1 point-group symmetry. All single-point calculations used the def2-TZVP basis set. Configuration and population analysis on CASSCF wave functions were done with localized orbitals by the Pipek–Mezey scheme, while Foster–Boys localization led to equivalent results.⁴⁹ This analysis was also performed on CASSCF/def2-SVP wave functions, and similar results were observed. Active spaces contained six electrons in five MOs (6e,5o) for H_2Succ , (8e,6o) for H_2Succ^- , and (12e,10o) for MNAH reactions as determined from analysis of occupation numbers and selection of reactive MOs. As MOs may change shape and ordering along the reaction path, CASSCF calculations started from the geometry with highest multi-configurational character (product for H_2Succ and reactant for H_2Succ^- and MNAH reactions), and guess MOs were taken from the CASSCF calculation of an adjacent geometry along the path.

The short-range influence of the enzymatic environment on the mechanism of flavin-mediated oxidation was emulated with truncated active site models (Figure S1, Supporting Information). For succinate oxidation catalyzed by respiratory complex II, the model contained 192 atoms including FAD (for which the ribityl-ADP moiety was replaced by 2-hydroxyethyl), succinate (deprotonated, $Succ^-$), side chains of H365, T377, E378, R402, H504, and R544, backbones of G170 and G546, and eight water molecules, which compose the first coordination shell around the flavin and substrate groups. The initial model structure was based on the PDB ID 1Y0P³⁸ from *F. frigidimarina* fumarate reductase flavoprotein, homologous to the respiratory complex II. This complete enzyme bound to succinate was solvated, neutralized, and equilibrated for 22 ns of classical molecular dynamics simulation, using the CHARMM36 force field.⁵⁰ The listed groups were extracted from this equilibrated structure, and dangling covalent bonds were saturated by hydrogen atoms. Reactive geometries were obtained by relaxed potential energy surface scans along the same reaction coordinate defined above (RC) with position restraints applied to C_α or C_β of capped amino acids to preserve the active site architecture. This corresponds to the H_2Succ reaction in Figure 2B.

For NADH oxidation catalyzed by respiratory complex I, the active site model contained 167 atoms including FMN, NADH (for which phosphate group and ADP moiety were replaced by methyl groups), side chains of residues N92, E97, Y180, N220, S295, and T325, and backbone of residues G183 and E184 from the Nqo1 subunit of *T. thermophilus* complex I as found in the PDB ID 3IAM³⁵ structure. This model corresponds to the MNAH reaction in Figure 2A. Geometries of stationary

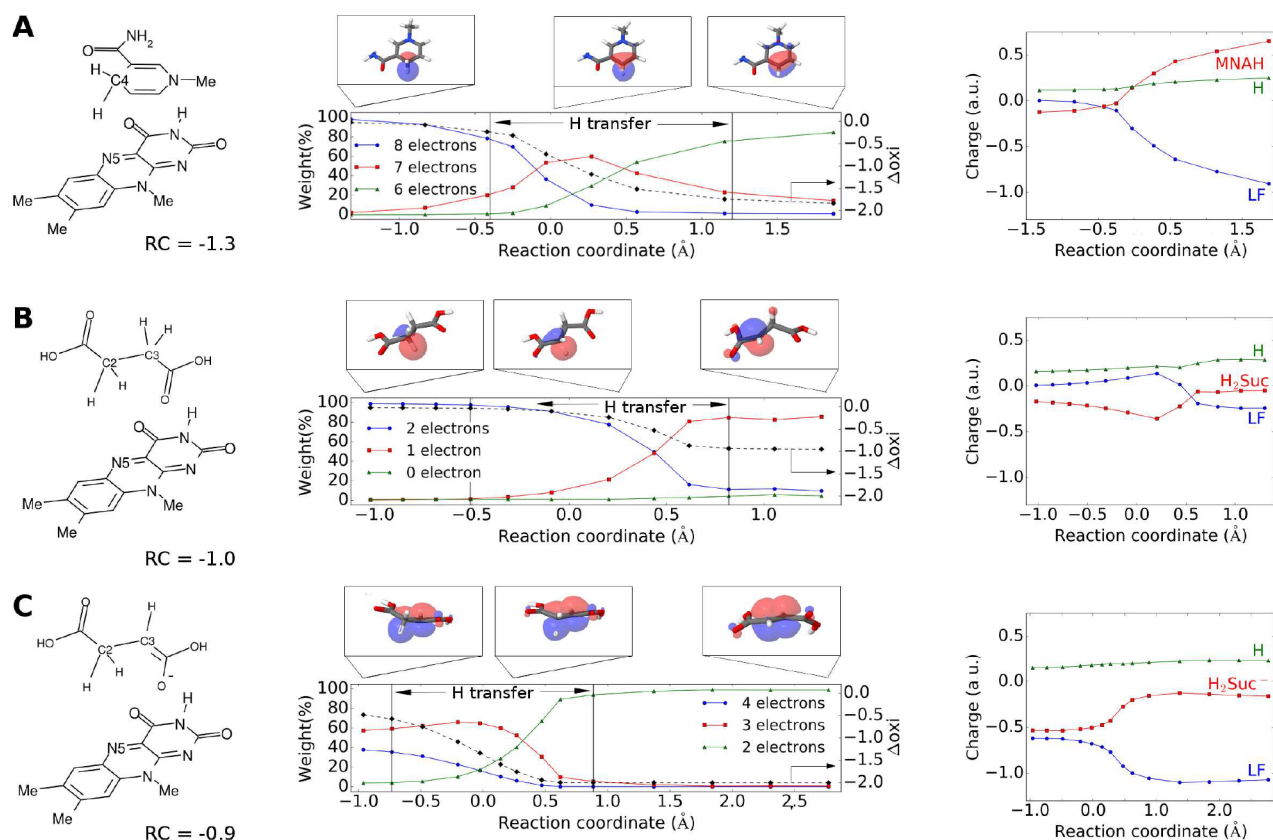


Figure 2. Mechanisms of flavin mediated oxidation from analysis of the wave function along the reaction. Panels A, B, and C show the reactions studied here, corresponding respectively to steps (a), (b), and (c) in Figure 1. The left column presents the reactant states. The middle column shows the contribution or weight of wave function configurations with n -electrons in molecular orbitals (MOs) localized in the donor along the proton-transfer reaction coordinate. Δ_{oxi} is calculated from eq 1 and shown in the dashed line. In the H transfer range, the transferred hydrogen is not fully bound to either donor or acceptor. The broken C–H bond σ MO is shown on top, and the lone-pair MO is also shown for H₂Suc⁻. The right column shows Mulliken partial charges for the transferred H, flavin, and donor groups.

points were optimized in the B3LYP-D3/def2-SVP level⁵¹ and kindly provided by Prof. Ville Kaila from their original study.²⁷ Geometries for the complex II model were optimized at the M06-L/def2-SVP level.⁵² Geometries of the enzyme models showed little dependency on the optimization level if dispersion interactions were accounted for (as in B3LYP-D3 or M06-L functionals). Wave functions for stationary points were obtained at the CASSCF/def2-SVP level with the same active spaces used for the isolated reactions.

RESULTS AND DISCUSSION

Three model reactions corresponding to steps (a)–(c) in Figure 1 were studied with a lumiflavin (LF, R_1 = methyl) acceptor, NADH modeled as 1-methylnicotinamide (MNAH), and succinate protonated to H₂Suc (succinic acid) for E1 elimination and H₂Suc⁻ (carbanion \leftrightarrow enolate electromer) for E1cb elimination. See panels A, B, and C in Figure 2 for the reactant structures, consistent with enzymatic active sites.

In order to quantify the extent of electron transfer along the reaction and avoid the pitfalls of using only partial charges to analyze PCET mechanisms,^{29,33} we propose a simple quantitative diagnostic of electron transfer employing weights of wave function configurations constructed with orbitals localized in the donor. This electronic charge transferred, Δ_{oxi} , is defined along the reaction coordinate (RC) as

$$\Delta_{oxi}(\text{RC}) = \sum_n n w_n(\text{RC}) - \max\{n\} \quad (1)$$

where n is the number of electrons occupying active MOs localized in the donor, $\max\{n\}$ is their maximum occupation at the reactant state, and w_n is the combined weight of wave function configurations with n -electrons. Only configurations with $w_n > 1\%$ in at least one geometry along the reaction were considered. This analysis may be used with any kind of multiconfigurational wave function obtained with localized MOs.⁴¹

We start with the H₂Suc reaction (model for succinate E1 elimination, Figure 2B) in which the broken C–H bond σ MO becomes a nonbonding MO in the product. This is the only active MO localized in the H₂Suc donor, thus $\{n\} = (0, 1, 2)$ electrons and $\max\{n\} = 2$. Figure 2B middle column shows that the contribution (combined weight) to the wave function of this localized MO changes from almost 100% for two-electron occupation in the reactant to 80% for one-electron occupation in the product. The average electronic charge transferred is $\Delta_{oxi} = -1$, showing that the H₂Suc reaction is a hydrogen-atom transfer (HAT).

In the biradical product, an unpaired electron occupies the LF π^* MO and spin-couples to a singlet state with the unpaired electron in the carbocation (Figure 2B, top of middle column), resulting in a short distance ($r_1 = 2.3$ Å) between the two molecules. Interestingly, this is in line with experimental

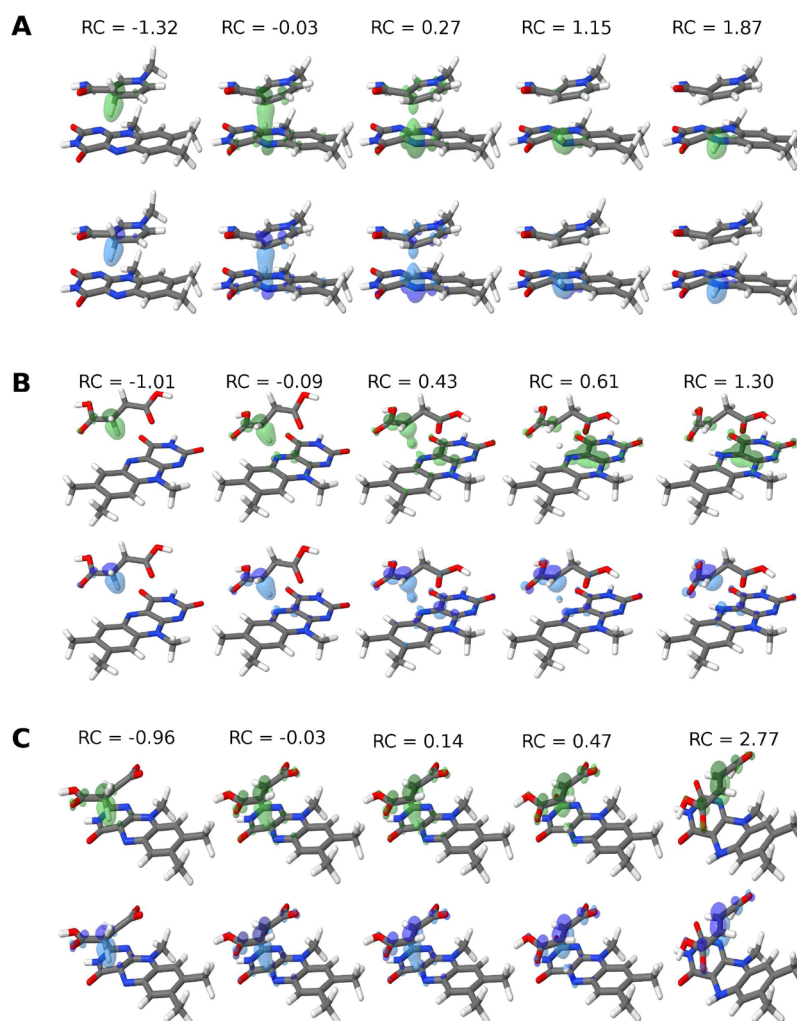


Figure 3. Intrinsic bond orbitals of the broken C–H bond for geometries with a given reaction coordinate (RC) along the pathway for MNAH (A), H₂Suc (B), and H₂Suc[−] (C) oxidation. Green α and blue β spin-orbitals are shown.

observation of a FAD flavosemiquinone radical signal during the catalytic cycle of respiratory complex II.⁵³

Partial charges condensed on the LF and H₂Suc groups are similar (within $0.2e$, Figure 2B, right column) and nearly neutral when comparing reactant and product (end) states, suggesting there is no net charge separation or redistribution, in accordance to a HAT.^{13,15} The partial charge on the transferred H atom is close to $0.2e$ along the complete pathway for all reactions studied here (Figure 2, right column). A naive interpretation of this partial charge would suggest a HAT is observed in all reactions, but this is not the case as clearly shown for the other two reactions below.

For H₂Suc[−] (E1cb elimination, Figure 2C), the nonbonding MO with the extra electron lone-pair and the σ MO of the broken C–H bond localize in the donor. Only configurations with $\{n\} = (2, 3, 4)$ electrons in these orbitals contribute significantly (more than 1%) to the wave function, thus $\max\{n\} = 4$. Remarkably, the anionic reactant already shows a substantial charge transfer ($\Delta\text{oxi} = -0.5$ at RC = -1.0 Å). When fumaric acid is formed, only configurations with two electrons in the forming double bond become relevant, resulting in a much longer distance ($r_1 = 3.8$ Å) between LF[−] and fumaric acid. The average $\Delta\text{oxi} = -2$ in the product, and this reaction is clearly a hydride transfer. Partial charges

change considerably between end states, and LF has a $-1e$ charge in the product, as expected from receiving a hydride.

For the MNAH reaction (Figure 2A), the MO of the broken C–H bond becomes a π MO and conjugates with the other nicotinamide MOs. A total of six active MOs are localized in the donor. Only configurations with $\{n\} = (6, 7, 8)$ electrons in these orbitals contribute significantly to the wave function, thus $\max\{n\} = 8$. Weights change from almost 100% for configurations with eight electrons in the reactant state to 85% for six electrons in the product, with a final $\Delta\text{oxi} \approx -2$. We conclude this reaction is also a hydride transfer.

It is noteworthy that weights for configurations with an odd number of electrons localized in the donor (one electron for H₂Suc, three for H₂Suc[−], and seven for MNAH reactions) peak near the transition state (TS, RC = -0.03 Å for MNAH, 0.61 Å for H₂Suc, and 0.14 Å for H₂Suc[−], Table S1). This is in line with $\Delta\text{oxi} \approx -1$ at the TS for the three reactions (Figure 2, middle column) and suggests that the activation energies correspond to the first (and only in H₂Suc reaction) electron transfer. Partial charge or other population analysis^{30–32} cannot usually provide this level of detail.

Electron and proton transfer occur concerted along the same range of reaction coordinates for the three studied reactions (H transfer indicated in Figure 2). However, analysis of intrinsic bond orbitals (IBO,^{32,33} Figure 3A) suggests that the

two transfers take place from (or to) the same donor (acceptor) site only for the MNAH reaction as orbitals (and the corresponding electron density) from the C–H bond in the reactant turn into the N5–H bond in the product after H[−] transfer. On the other hand, electron and proton transfer in the two succinic acid reactions proceed to different sites of the acceptor flavin. These two reactions should be classified as concerted PCET^{11,13} or multiple-site PCET¹⁴ as orbitals of the broken C–H bond in the reactant do not turn into the N5–H bond in the product. For the H₂Suc reaction, the one electron transferred from the broken C–H bond to the flavin delocalizes over the pyrimidinedione ring (Figure 3B). For the H₂Suc[−] reaction, the broken C–H bond rearranges to form the double bond in fumaric acid (Figure 3C), and the two electrons transferred to flavin come from the nonbonding MO with the extra electron lone-pair (Figure S2).

Finally, we tested whether the mechanisms observed above are conserved in the enzymatic environment. Truncated active site models with 167 and 192 atoms, respectively, coordinating NADH in respiratory complex I and succinate in respiratory complex II were built from these protein crystallographic structures (Figure S1).^{35,37,38} Analysis of Δoxi (eq 1) calculated for these active site models using the same methods depicted above shows NADH oxidation proceeds via hydride transfer, and succinate oxidation in E1 elimination occurs through HAT (Table S2), showing that the enzymatic mechanisms are equivalent to those of the isolated models.

CONCLUSIONS

We confirm the traditional view³⁶ that NADH oxidation by flavin proceeds via a prototypical hydride transfer, with the two electrons moving concerted with the proton from the donor to the same acceptor group. A previous proposal of HAT for this reaction²⁷ is incorrect and illustrates the pitfalls of assigning PCET mechanisms with diagnostics based only on partial charges. For succinate oxidation by flavin, two reaction sequences are possible. E1 elimination may occur by a HAT, opposed to usual proposals,³⁹ but E1cb elimination will also proceed via hydride with an advanced charge transfer in the reactant state.

PCET mechanisms of flavin-mediated oxidation depend on the donor molecule. This should have implications for the mechanisms of several flavoproteins besides those of the respiratory chain studied here. It is also expected that the simple diagnostic of electron transfer along the reaction pathway proposed here will be useful to characterize a broad class of PCET processes.

ASSOCIATED CONTENT

Supporting Information

The Supporting Information is available free of charge at <https://pubs.acs.org/doi/10.1021/acs.jcim.0c00945>.

Two figures with the structure of truncated enzyme active site models and additional IBO analysis and two tables with quantification of electron transfer (Δoxi) for enzyme models and TS analysis. (PDF)

AUTHOR INFORMATION

Corresponding Author

Guilherme M. Arantes – Department of Biochemistry, Instituto de Química, Universidade de São Paulo, 05508-900 São Paulo,

SP, Brazil; orcid.org/0000-0001-5356-7703;
Email: garantes@iq.usp.br

Author

Felipe Curtolo – Department of Biochemistry, Instituto de Química, Universidade de São Paulo, 05508-900 São Paulo, SP, Brazil; orcid.org/0000-0002-4459-0968

Complete contact information is available at:
<https://pubs.acs.org/10.1021/acs.jcim.0c00945>

Notes

The authors declare no competing financial interest.

ACKNOWLEDGMENTS

Fruitful discussions with Prof. Peter R. Taylor and funding from Fundação de Amparo à Pesquisa do Estado de São Paulo (FAPESP, scholarships 2016/23525-0 and 2017/26109-0 to F.C. and Grants 2016/24096-5 and 2019/21856-7 to G.M.A.) are gratefully acknowledged.

REFERENCES

- (1) Joosten, V.; van Berkel, W. J. Flavoenzymes. *Curr. Opin. Chem. Biol.* **2007**, *11*, 195–202.
- (2) Sobrado, P.; Gadda, G. Introduction to Flavoproteins: Beyond the Classical Paradigms. *Arch. Biochem. Biophys.* **2017**, *632*, 1–3.
- (3) Gray, M.; Goodman, A. J.; Carroll, J. B.; Bardon, K.; Markey, M.; Cooke, G.; Rotello, V. M. Model Systems for Flavoenzyme Activity: Interplay of Hydrogen Bonding and Aromatic Stacking in Cofactor Redox Modulation. *Org. Lett.* **2004**, *6*, 385–388.
- (4) Nandwana, V.; Samuel, I.; Cooke, G.; Rotello, V. M. Aromatic Stacking Interactions in Flavin Model Systems. *Acc. Chem. Res.* **2013**, *46*, 1000–1009.
- (5) Reis, A. A. O.; Sayegh, R. S. R.; Marana, S. R.; Arantes, G. M. Combining Free Energy Simulations and NMR Chemical-Shift Perturbation To Identify Transient Cation- π Contacts in Proteins. *J. Chem. Inf. Model.* **2020**, *60*, 890–897.
- (6) Chaiyen, P.; Scrutton, N. S. Flavins and Flavoproteins. *FEBS J.* **2015**, *282*, 3001–3002.
- (7) Bresnahan, C. G.; Reinhardt, C. R.; Bartholow, T. G.; Rumpel, J. P.; North, M.; Bhattacharyya, S. Effect of Stacking Interactions on the Thermodynamics and Kinetics of Lumiflavin: A Study with Improved Density Functionals and Density Functional Tight-Binding Protocol. *J. Phys. Chem. A* **2015**, *119*, 172–182.
- (8) Buckel, W.; Thauer, R. K. Flavin-Based Electron Bifurcation, A New Mechanism of Biological Energy Coupling. *Chem. Rev.* **2018**, *118*, 3862–3886.
- (9) Cukier, R. I.; Nocera, D. G. Proton-Coupled Electron Transfer. *Annu. Rev. Phys. Chem.* **1998**, *49*, 337–369.
- (10) Huynh, M. H. V.; Meyer, T. J. Proton-Coupled Electron Transfer. *Chem. Rev.* **2007**, *107*, 5004–5064.
- (11) Warren, J. J.; Tronic, T. A.; Mayer, J. M. Thermochemistry of Proton-Coupled Electron Transfer Reagents and its Implications. *Chem. Rev.* **2010**, *110*, 6961–7001.
- (12) Hammes-Schiffer, S. Comparison of Hydride, Hydrogen Atom, and Proton-Coupled Electron Transfer Reactions. *ChemPhysChem* **2002**, *3*, 33–42.
- (13) Hammes-Schiffer, S. Proton-Coupled Electron Transfer: Classification Scheme and Guide to Theoretical Methods. *Energy Environ. Sci.* **2012**, *5*, 7696–7703.
- (14) Darcy, J. W.; Koronkiewicz, B.; Parada, G. A.; Mayer, J. M. A Continuum of Proton-Coupled Electron Transfer Reactivity. *Acc. Chem. Res.* **2018**, *51*, 2391–2399.
- (15) Hammes-Schiffer, S.; Stuchebrukhov, A. A. Theory of Coupled Electron and Proton Transfer Reactions. *Chem. Rev.* **2010**, *110*, 6939–6960.

- (16) Brenner, S.; Hay, S.; Heyes, D. J.; Scrutton, N. S. *Proton-Coupled Electron Transfer: A Carrefour of Chemical Reactivity Traditions*; The Royal Society of Chemistry, 2012; pp 57–88.
- (17) Poulsen, T. D.; Garcia-Viloca, M.; Gao, J.; Truhlar, D. G. Free Energy Surface, Reaction Paths, and Kinetic Isotope Effect of Short-Chain Acyl-CoA Dehydrogenase. *J. Phys. Chem. B* **2003**, *107*, 9567–9578.
- (18) Bhattacharyya, S.; Stankovich, M. T.; Truhlar, D. G.; Gao, J. Combined Quantum Mechanical and Molecular Mechanical Simulations of One- and Two-Electron Reduction Potentials of Flavin Cofactor in Water, Medium-Chain Acyl-CoA Dehydrogenase, and Cholesterol Oxidase. *J. Phys. Chem. A* **2007**, *111*, 5729–5742.
- (19) Pang, J.; Hay, S.; Scrutton, N. S.; Sutcliffe, M. J. Deep Tunneling Dominates the Biologically Important Hydride Transfer Reaction from NADH to FMN in Morphinone Reductase. *J. Am. Chem. Soc.* **2008**, *130*, 7092–7097.
- (20) Delgado, M.; Görlich, S.; Longbotham, J. E.; Scrutton, N. S.; Hay, S.; Moliner, V.; Tuñón, I. Convergence of Theory and Experiment on the Role of Preorganization, Quantum Tunneling, and Enzyme Motions into Flavoenzyme-Catalyzed Hydride Transfer. *ACS Catal.* **2017**, *7*, 3190–3198.
- (21) Tan, S. L. J.; Novianti, M. L.; Webster, R. D. Effects of Low to Intermediate Water Concentrations on Proton-Coupled Electron Transfer (PCET) Reactions of Flavins in Aprotic Solvents and a Comparison with the PCET Reactions of Quinones. *J. Phys. Chem. B* **2015**, *119*, 14053–14064.
- (22) Mathes, T.; Zhu, J.; van Stokkum, I. H. M.; Groot, M. L.; Hegemann, P.; Kennis, J. T. M. Hydrogen Bond Switching among Flavin and Amino Acids Determines the Nature of Proton-Coupled Electron Transfer in BLUF Photoreceptors. *J. Phys. Chem. Lett.* **2012**, *3*, 203–208.
- (23) Goings, J. J.; Hammes-Schiffer, S. Early Photocycle of Slr1694 Blue-Light Using Flavin Photoreceptor Unraveled through Adiabatic Excited-State Quantum Mechanical/Molecular Mechanical Dynamics. *J. Am. Chem. Soc.* **2019**, *141*, 20470–20479.
- (24) Soudackov, A. V.; Hammes-Schiffer, S. Probing Non-adiabaticity in the Proton-Coupled Electron Transfer Reaction Catalyzed by Soybean Lipoygenase. *J. Phys. Chem. Lett.* **2014**, *5*, 3274–3278.
- (25) Sirjoosingh, A.; Hammes-Schiffer, S. Proton-Coupled Electron Transfer versus Hydrogen Atom Transfer: Generation of Charge-Localized Diabatic States. *J. Phys. Chem. A* **2011**, *115*, 2367–2377.
- (26) Abe, Y.; Shoji, M.; Nishiyama, Y.; Aiba, H.; Kishimoto, T.; Kitaura, K. The Reaction Mechanism of Sarcosine Oxidase Elucidated Using FMO and QM/MM Methods. *Phys. Chem. Chem. Phys.* **2017**, *19*, 9811–9822.
- (27) Saura, P.; Kaila, V. R. I. Energetics and Dynamics of Proton-Coupled Electron Transfer in the NADH/FMN Site of Respiratory Complex I. *J. Am. Chem. Soc.* **2019**, *141*, 5710–5719.
- (28) Arantes, G. M.; Bhattacharjee, A.; Field, M. J. Homolytic Cleavage of Fe–S Bonds in Rubredoxin Under Mechanical Stress. *Angew. Chem., Int. Ed.* **2013**, *52*, 8144–8146.
- (29) Politzer, P.; Harris, R. R. Properties of Atoms in Molecules. I. Proposed Definition of the Charge on an Atom in a Molecule. *J. Am. Chem. Soc.* **1970**, *92*, 6451–6454.
- (30) Reed, A. E.; Weinstock, R. B.; Weinhold, F. Natural Population Analysis. *J. Chem. Phys.* **1985**, *83*, 735–746.
- (31) Martin, F.; Zipse, H. Charge Distribution in the Water Molecule - A Comparison of Methods. *J. Comput. Chem.* **2005**, *26*, 97–105.
- (32) Knizia, G. Intrinsic Atomic Orbitals: An Unbiased Bridge between Quantum Theory and Chemical Concepts. *J. Chem. Theory Comput.* **2013**, *9*, 4834–4843.
- (33) Klein, J. E. M. N.; Knizia, G. cPCET versus HAT: A Direct Theoretical Method for Distinguishing X-H Bond-Activation Mechanisms. *Angew. Chem., Int. Ed.* **2018**, *57*, 11913–11917.
- (34) Mandal, M.; Elwell, C. E.; Bouchev, C. J.; Zerk, T. J.; Tolman, W. B.; Cramer, C. J. Mechanisms for Hydrogen-Atom Abstraction by Mononuclear Copper(III) Cores: Hydrogen-Atom Transfer or Concerted Proton-Coupled Electron Transfer? *J. Am. Chem. Soc.* **2019**, *141*, 17236–17244.
- (35) Berrisford, J. M.; Sazanov, L. A. Structural Basis for the Mechanism of Respiratory Complex I. *J. Biol. Chem.* **2009**, *284*, 29773–29783.
- (36) Hirst, J. Mitochondrial Complex I. *Annu. Rev. Biochem.* **2013**, *82*, 551–575.
- (37) Teixeira, M. H.; Arantes, G. M. Balanced Internal Hydration Discriminates Substrate Binding to Respiratory Complex I. *Biochim. Biophys. Acta, Bioenerg.* **2019**, *1860*, 541–548.
- (38) Wardrope, C.; Mowat, C. G.; Walkinshaw, M. D.; Reid, G. A.; Chapman, S. K. Fumarate Reductase: Structural and Mechanistic Insights from the Catalytic Reduction of 2-methylfumarate. *FEBS Lett.* **2006**, *580*, 1677–1680.
- (39) Maklashina, E.; Cecchini, G.; Dikanov, S. A. Defining a Direction: Electron Transfer and Catalysis in Escherichia coli Complex II Enzymes. *Biochim. Biophys. Acta, Bioenerg.* **2013**, *1827*, 668–678.
- (40) Lucas, M. F.; Ramos, M. J. Mechanism of a Soluble Fumarate Reductase from *Shewanella frigidimarina*: A Theoretical Study. *J. Phys. Chem. B* **2006**, *110*, 10550–10556.
- (41) Helgaker, T.; Jørgensen, P.; Olsen, J. *Molecular Electronic-Structure Theory*, 1st ed.; Wiley: New York, 2000.
- (42) Weigend, F.; Ahlrichs, R. Balanced Basis Sets of Split Valence, Triple Zeta Valence and Quadruple Zeta Valence Quality for H to Rn: Design and Assessment of Accuracy. *Phys. Chem. Chem. Phys.* **2005**, *7*, 3297–3305.
- (43) Weigend, F. Accurate Coulomb-Fitting Basis Sets for H to Rn. *Phys. Chem. Chem. Phys.* **2006**, *8*, 1057–1065.
- (44) Hellweg, A.; Hättig, C.; Höfener, S.; Klopper, W. Optimized Accurate Auxiliary Basis Sets for RI-MP2 and RI-CC2 Calculations for the Atoms Rb to Rn. *Theor. Chem. Acc.* **2007**, *117*, 587–597.
- (45) Fukui, K. The Path of Chemical Reactions - The IRC Approach. *Acc. Chem. Res.* **1981**, *14*, 363–368.
- (46) Neese, F. Software Update: The ORCA Program System, Version 4.0. *Wiley Interdiscip. Rev.: Comput. Mol. Sci.* **2018**, *8*, No. e1327.
- (47) Zhao, Y.; Truhlar, D. G. The M06 Suite of Density Functionals for Main Group Thermochemistry, Thermochemical Kinetics, Noncovalent Interactions, Excited States, and Transition Elements: Two New Functionals and Systematic Testing of Four M06-Class Functionals and 12 Other Functionals. *Theor. Chem. Acc.* **2008**, *120*, 215–241.
- (48) Sun, Q.; Berkelbach, T. C.; Blunt, N. S.; Booth, G. H.; Guo, S.; Li, Z.; Liu, J.; McClain, J. D.; Sayfutyarova, E. R.; Sharma, S.; Wouters, S.; Chan, G. K.-L. PySCF: The Python-based Simulations of Chemistry Framework. *Wiley Interdiscip. Rev.: Comput. Mol. Sci.* **2018**, *8*, No. e1340.
- (49) Pipek, J.; Mezey, P. A Fast Intrinsic Localization Procedure Applicable for ab Initio and Semiempirical Linear Combination of Atomic Orbital Wave Functions. *J. Chem. Phys.* **1989**, *90*, 4916–4926.
- (50) Huang, J.; MacKerell, A. D., Jr. CHARMM36 All-Atom Additive Protein Force Field: Validation Based on Comparison to NMR Data. *J. Comput. Chem.* **2013**, *34*, 2135–2145.
- (51) Becke, A. D. Density Functional Thermochemistry. III. The Role of Exact Exchange. *J. Chem. Phys.* **1993**, *98*, 5648.
- (52) Zhao, Y.; Truhlar, D. G. A New Local Density Functional for Main-Group Thermochemistry, Transition Metal Bonding, Thermochemical Kinetics, and Noncovalent Interactions. *J. Chem. Phys.* **2006**, *125*, 194101.
- (53) Maklashina, E.; Iverson, T. M.; Sher, Y.; Kotlyar, V.; Andréll, J.; Mirza, O.; Hudson, J. M.; Armstrong, F. A.; Rothery, R. A.; Weiner, J. H.; Cecchini, G. Fumarate Reductase and Succinate Oxidase Activity of Escherichia coli Complex II Homologs Are Perturbed Differently by Mutation of the Flavin Binding Domain. *J. Biol. Chem.* **2006**, *281*, 11357–11365.